

# Concentration and mobility of mobile $\text{Li}^+$ ions in $\text{Li}_6\text{BaLa}_2\text{Ta}_2\text{O}_{12}$ and $\text{Li}_5\text{La}_3\text{Ta}_2\text{O}_{12}$ garnet lithium ion conductors

Mohamad M. Ahmad<sup>1,2</sup> · Abdullah Al-Jaafari<sup>1</sup>

Received: 15 April 2015 / Accepted: 7 July 2015 / Published online: 11 July 2015  
© Springer Science+Business Media New York 2015

**Abstract** The concentration of mobile ions,  $n_c$ , and their mobility are important factors that control the conduction process in ionic conductors. The analysis of the conductivity spectra of  $\text{Li}_6\text{BaLa}_2\text{Ta}_2\text{O}_{12}$  (LBLT) and  $\text{Li}_5\text{La}_3\text{Ta}_2\text{O}_{12}$  (LLT)  $\text{Li}^+$  conducting garnets at low temperatures helps us to estimate the values of  $n_c$  of  $\text{Li}^+$  ions and their mobility. We found that  $n_c$  is independent of temperature with an average values of  $1.93 \times 10^{21}$  and  $6.71 \times 10^{20} \text{ cm}^{-3}$  for LBLT and LLT, respectively. These values of  $n_c$  represent only a small fraction of 8.79 % (in LBLT) and 3.52 % (in LLT) out of the total  $\text{Li}^+$  ions content. Our results confirm that the conduction process is controlled by the mobility of  $\text{Li}^+$  ions, which is related to the occupancy of  $\text{Li}^+$  in the tetrahedral sites of the garnet phases. Moreover, the diffusivity of  $\text{Li}^+$  has been estimated at different temperatures and compared to other fast  $\text{Li}^+$  conductors.

## 1 Introduction

Rechargeable lithium ion batteries have been developed as the next-generation high-performance power sources in various electronic devices, such as portable, computing, telecommunicating and entertainment equipments [1, 2]. However, the current commercial Li batteries suffers from several drawbacks including large capacity loss, poor electrochemical stability, limited temperature range of

operation and safety concerns due to the use of flammable organic/polymer-based  $\text{Li}^+$  ion conductors as electrolytes [3, 4]. Therefore, using ceramic/inorganic lithium solid electrolytes has been proposed for the development of all solid-state lithium-ion batteries. Solid Li electrolytes should exhibit high bulk ionic conductivity in the  $10^{-3}$  S/cm range at room temperature, low grain boundary resistance and good chemical stability on contact with Li metal electrodes [3, 4].

Solid Li ion conductors with the garnet-like structure of the formula  $\text{Li}_5\text{La}_3\text{M}_2\text{O}_{12}$  ( $\text{M} = \text{Ta}, \text{Nb}$ ) show negligible electronic conductivity, have good ionic conductivity in the range of  $10^{-6}$  S/cm at room temperature with small contribution from the grain boundaries [4–8]. These garnet materials are also stable against reaction with metallic lithium and are stable in air at ambient and high temperatures. These features make lithium conducting garnets promising candidates for applications in solid-state lithium ion batteries. Considerable enhancement of the ionic conductivity of the lithium garnet materials has been achieved by chemical substitutions and structural modifications [4–20].  $\text{Li}_6\text{BaLa}_2\text{Ta}_2\text{O}_{12}$  and the cubic phase of  $\text{Li}_7\text{La}_3\text{Zr}_2\text{O}_{12}$  garnets, for example, have ionic conductivity value of  $10^{-5}$ – $10^{-4}$  S/cm at room temperature [4, 9]. Ionic conductivity value of  $8 \times 10^{-4}$  and  $1 \times 10^{-3}$  S/cm at room temperature has been reported for  $\text{Li}_{6.75}\text{La}_3\text{Zr}_{1.75}\text{Nb}_{0.25}\text{O}_{12}$  and  $\text{Li}_{6.4}\text{La}_3\text{Zr}_{1.4}\text{Ta}_{0.6}\text{O}_{12}$  garnets, respectively [15, 16]. In order to develop new fast lithium ion conducting garnets it is essential to understand the crystal structure and the lithium conduction mechanism. Despite the extensive work on the crystal structure and the lithium conduction mechanism in garnet materials, there is no information on the concentration and mobility of  $\text{Li}^+$  ions in these materials. Therefore, the purpose of the present work is to estimate the concentration and the mobility of mobile  $\text{Li}^+$  in garnet materials.

✉ Mohamad M. Ahmad  
mmohamad@kfu.edu.sa; mmahmad@aun.edu.eg

<sup>1</sup> Department of Physics, College of Science, King Faisal University, Al-Ahsaa 31982, Saudi Arabia

<sup>2</sup> Physics Department, Faculty of Science, Assiut University in The New Valley, El-Kharga 72511, Egypt

## 2 Experiment

Li<sub>6</sub>BaLa<sub>2</sub>Ta<sub>2</sub>O<sub>12</sub> (LBLT) powder was prepared by a combination of mechanical milling and solid state reaction techniques. Stoichiometric amounts of Li<sub>2</sub>CO<sub>3</sub> (10 wt% excess of Li<sub>2</sub>CO<sub>3</sub> was added to compensate for lithium loss at high temperatures), BaCO<sub>3</sub>, Ta<sub>2</sub>O<sub>5</sub> and La<sub>2</sub>O<sub>3</sub> (dried at 900 °C overnight) were ball milled for 12 h in 2-propanole in tungsten carbide media with a rotation speed of 350 rpm. The dried powder was calcinated at 700 °C for 12 h, then ball milled again for 6 h. A second calcination step at 775 °C for 9 h was performed followed by a final ball milling process at 400 rpm for 4 h. LBLT ceramics were obtained by sintering the green pellets at 800 and 900 °C for 12 h. Li<sub>5</sub>La<sub>3</sub>Ta<sub>2</sub>O<sub>12</sub> (LLT) is prepared using the same techniques with a single calcination step at 700 °C for 12 h. Before and after the heat treatment the powder was ball milled for 12 h in 2-propanole. LLT ceramics were obtained by sintering the green pellets at 975 °C for 12 h. The product materials were characterized by powder X-ray diffraction (XRD) and scanning electron microscopy for structural analysis. Impedance spectroscopy (IS) measurements were performed on the sintered materials using Novocontrol concept 50 system in the 1–10<sup>7</sup> Hz frequency range. The measurements were performed in the 180–400 K temperature range, where the temperature was controlled by the Quatro cryosystem.

## 3 Results and discussion

The XRD patterns of the sintered LBLT and LLT samples are shown in Fig. 1. The observed patterns agree with the standard XRD data of Li<sub>5</sub>La<sub>3</sub>Ta<sub>2</sub>O<sub>12</sub> (JCPDS No. 45-0110), indicating the formation of the cubic garnet structure with no secondary phases. The SEM micrograph of LBLT sample sintered at 800 °C is shown in Fig. 2a. Cube-like

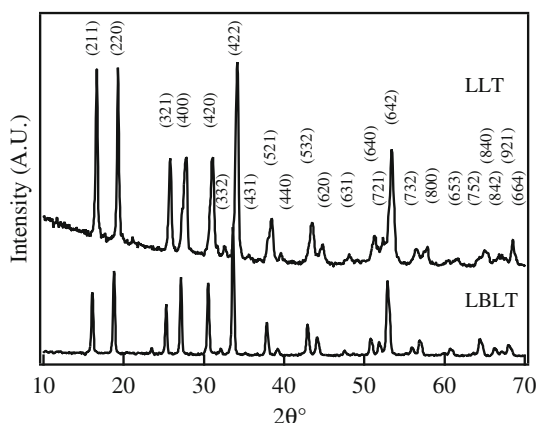


**Fig. 1** Powder X-ray diffraction patterns of Li<sub>6</sub>BaLa<sub>2</sub>Ta<sub>2</sub>O<sub>12</sub> and Li<sub>5</sub>La<sub>3</sub>Ta<sub>2</sub>O<sub>12</sub> garnet materials

grains are observed with a grain size of ~0.7 μm. However, high magnification of the SEM micrograph in Fig. 2b indicates that the sub-micrometer grains are actually formed from nano-sized grains of less than 100 nm size. The grain size of the studied materials increases to ~2 μm with increasing the sintering temperature to 900 °C (Fig. 2c). In this sample the nano-sized grains are completely consumed to form the larger uniform grains. LLT exhibits coarse grains of about 2 μm size as shown in Fig. 2d.

The electrical properties of the investigated materials have been studied through impedance spectroscopy measurements. Complex impedance diagrams of LBLT and LLT ceramics are shown in Fig. 3. The impedance data shows one, almost ideal, semicircle at high frequencies followed by a large spike at the low frequency region due to electrode polarization effects. Electrode polarization becomes more prominent with increasing temperature. The presence of the large spike of the electrode polarization at low frequencies indicates that the conduction process is primarily ionic. The impedance semicircle cannot be resolved to grain and grain boundary contributions; therefore the intercept of the semicircle with the real axis represents the total ionic conductivity. The temperature dependence of the lithium ionic conductivity of LBLT ceramics is shown in Fig. 4. LBLT sample exhibits ionic conductivity value of 5.09 × 10<sup>-5</sup> S/cm at 22 °C. This value is higher than the conductivity values reported by Awaka et al. and Kokal et al. of 1.3 × 10<sup>-5</sup> and 1.69 × 10<sup>-5</sup> S/cm at 25 °C, respectively [13, 14]. It is also slightly higher than the value of 4.0 × 10<sup>-5</sup> S/cm at 22 °C reported by Thangadurai and Weppner [4]. The enhanced conductivity of LBLT ceramics sintered at a low temperature of 800 °C may be due to the fine-grain structure of the present samples, which may facilitate the Li<sup>+</sup> ions conduction process [21, 22]. This is supported by the fact that the LBLT sample sintered at 900 °C with larger grain size has a slightly reduced conductivity of 4.7 × 10<sup>-5</sup> S/cm at 22 °C.

For comparison, the conductivity data of Li<sub>5</sub>La<sub>3</sub>Ta<sub>2</sub>O<sub>12</sub> material sintered at 975 °C for 12 h is shown in Fig. 4. We have sintered the LLT material at 900, 950, 975 and 1000 °C and have found that the LLT-975 sample exhibits the highest conductivity. LLT-975 has a total ionic conductivity value of 4.77 × 10<sup>-6</sup> S/cm at 22 °C, which is one order of magnitude smaller than that of LBLT. At low temperatures, however, the conductivity of LBLT is more than two orders of magnitude larger than that of LLT, as observed in Fig. 4. The conductivity data in Fig. 4 is fitted by the Arrhenius relation:

$$\sigma = \sigma_o \exp\left(-\frac{\Delta E}{kT}\right) \tag{1}$$

where  $\sigma_o$  is the pre-exponential factor,  $k$  is the Boltzman's constant and  $\Delta E$  is the activation energy for the ionic

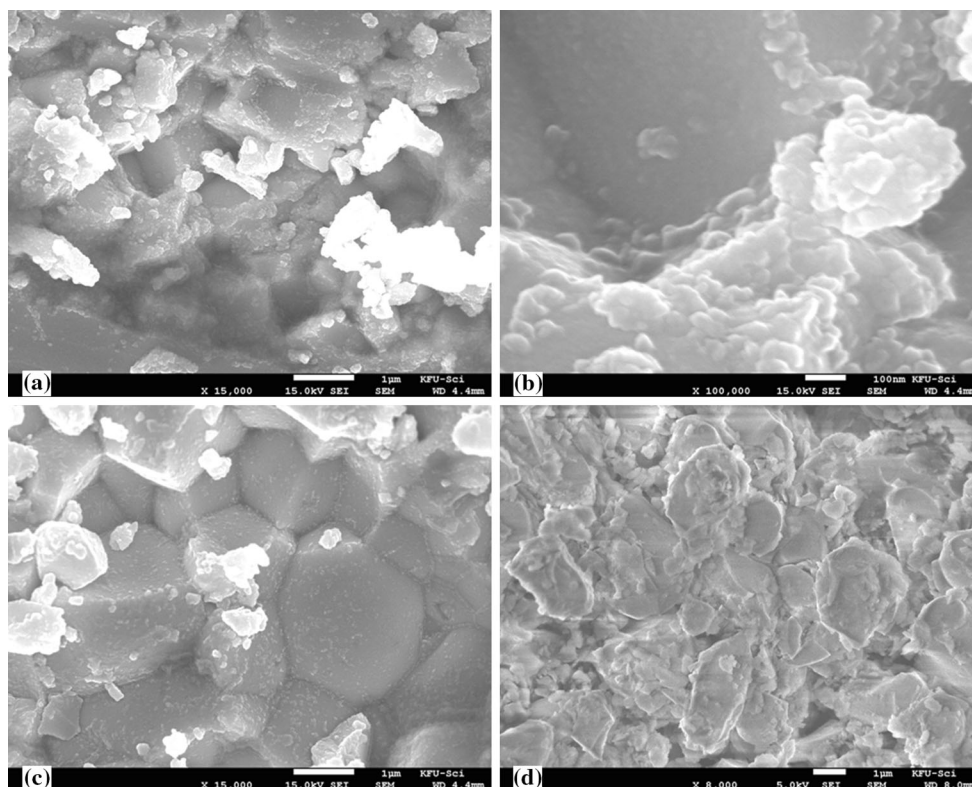


**Fig. 2** SEM micrographs of **a** LBLT-800, **b** high magnification for LBLT-800, **c** LBLT-900 and **d** LLT-975 ceramics

conduction. The value of the activation energy for LBLT is 0.43 eV, which is comparable to the previously reported values of 0.40–0.44 eV [4, 13, 14]. For LLT garnets, two straight-line regions with different values of the activation energy are observed. The values of  $\Delta E$  are 0.6 and 0.49 eV for the low-temperature (<340 K) and high-temperature regions, respectively.

In garnet materials the ionic conductivity increases with increasing  $\text{Li}^+$  ions per unit formula from 5 in  $\text{L}_5\text{La}_3\text{M}_2\text{O}_{12}$  ( $\text{M} = \text{Ta}, \text{Nb}, \text{Sb}, \text{Bi}$ ), 6 in  $\text{Li}_6\text{ALa}_2\text{M}_2\text{O}_{12}$  ( $\text{A} = \text{Ca}, \text{Sr}, \text{Ba}$ ) to 7  $\text{Li}^+$  ions per unit formula in the cubic  $\text{Li}_7\text{La}_3\text{Zr}_2\text{O}_{12}$ -based garnets.  $\text{Li}^+$  ions in the garnets occupy both the 24d tetrahedral sites and the 48g/96h octahedral sites. However, there is debate whether the  $\text{Li}^+$  ions in the tetrahedral or octahedral sites are mobile and contribute to the conduction process. While some studies suggested that  $\text{Li}^+$  ions in the tetrahedral sites are immobile and play no role in the conduction process [23–25], recent high temperature neutron diffraction and molecular dynamics calculations studies concluded that  $\text{Li}^+$  ions pathways involve both tetrahedral and octahedral sites [26, 27]. Xu et al. through ab initio calculations have indicated two possible pathways for  $\text{Li}^+$  ions transport: a long pathway (called route A, associated with high energy barrier of 0.8 eV) from one octahedral site to another octahedral site bypassing the 24d tetrahedral site [28]. The other shorter

pathway (route B, associated by a lower energy barrier of 0.26 eV) occurs by the hopping of  $\text{Li}^+$  ions between two octahedral sites via the 24d tetrahedral site [28]. Moreover, it is found that the occupancy of the tetrahedral and octahedral sites depends on lithium content [23, 24, 29]. With increasing lithium content O’Callaghan and Cussen have reported that the occupancy of 24d sites decreases whereas that of the octahedral sites increases [23, 24, 29]. The occupancy of the 24d sites and of the octahedral (48g and 96h) sites is 80 and 43 %, respectively for LLT, which changed to 67 and 64 %, respectively for LBLT [29].

Regardless of the vast number of studies on garnet lithium ion conductors there is no information on the concentration of mobile  $\text{Li}^+$  ions. In some reports the authors have estimated the total density ( $N$ ) of  $\text{Li}^+$  ions as the true concentration ( $n_c$ ) of  $\text{Li}^+$  mobile ions that are involved in the ionic conduction process, and have used the value of  $N$  to calculate the diffusivity of  $\text{Li}^+$  ions [18–20]. Actually, since a fraction of  $\text{Li}^+$  ions could be immobile [26, 27], then the value of  $n_c$  is expected to be smaller than that of  $N$ . In this work we estimate the values of  $n_c$  and the corresponding hopping frequency of mobile  $\text{Li}^+$  ions from the analysis of the conductivity spectra (the frequency dependence of the real part of the complex conductivity) at different temperatures [30–32]. The conductivity spectra are usually analyzed by a power-law model of the form [33],

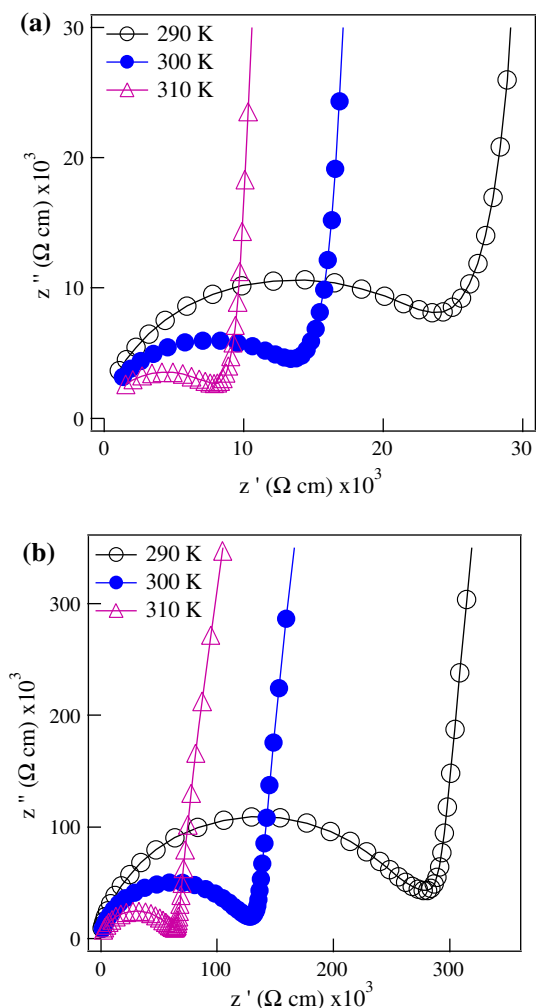


**Fig. 3** Complex impedance diagrams of **a** LBLT-800 and **b** LLT-975 at selected temperatures

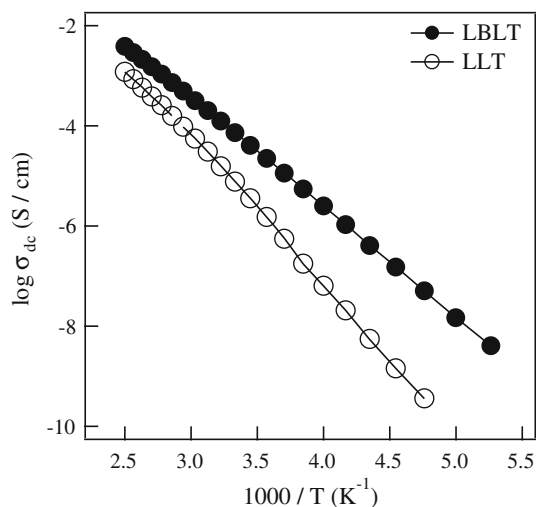


**Fig. 4** The temperature dependence of the dc conductivity of LBLT-800 and LLT-975 garnet materials

$$\sigma'(\omega) = \sigma_{dc} [1 + (\omega/\omega_c)^n], \tag{2}$$

where  $\sigma_{dc}$  is the dc conductivity,  $\omega$  is the angular frequency,  $n$  is the power-law exponent, and  $\omega_c$  is the crossover radial frequency from dc to the dispersive conductivity region. The dc conductivity in Eq. (2) could be given by the Nernst-Einstein relation;

$$\sigma_{dc} = en_c\mu = \frac{n_c e^2 \gamma \lambda^2}{kT} \omega_H, \tag{3}$$

where  $n_c$  is the concentration of mobile charge carriers,  $\mu$  is their mobility,  $e$  is the electronic charge,  $\gamma$  is a geometrical factor for ion hopping ( $\gamma = 1/6$  for isotropic conduction process),  $\lambda$  is the hopping distance, and  $\omega_H$  is the hopping frequency of mobile ions. It is clear from Eq. (3) that  $n_c$  and  $\mu$  (or equivalently  $\omega_H$ ) are the factors that control the dc conductivity. It is widely accepted in the literature that  $\omega_c$  of Eq. (2) represents a good estimate of the true hopping frequency of mobile ions [30–32]. Therefore, we have analyzed the conductivity spectra of the investigated materials using Eq. (2) in order to determine the values of  $\sigma_{dc}$  and  $\omega_c$ .

The fitting results of the conductivity spectra are shown as solid curves in Fig. 5a for LBLT. The extracted values of  $\sigma_{dc}$ ,  $\omega_c$  and  $n$  are listed in Table 1. The fitting process is limited to low temperatures because the conductivity dispersion region shifts out of our frequency window at high temperatures. The reciprocal temperature dependence of the dc conductivity  $\sigma_{dc}$  and the hopping frequency  $\omega_c$  obtained from the fitting process is shown in Fig. 6. The values of the activation energy for the ionic conduction,  $E_\sigma$ , and for ion hopping,  $E_H$ , determined from Fig. 6 are 0.44 and 0.45 eV, respectively. The close agreement between  $E_\sigma$  and  $E_H$  indicates that the concentration of mobile  $\text{Li}^+$  ions is independent of temperature [30–32].

We have estimated the values of the concentration of mobile  $\text{Li}^+$  ions,  $n_c$ , in the investigated materials by using Eq. (3). In this equation a value of the hopping distance as short as  $\lambda = 1.7 \text{ \AA}$  has been used [34]. The estimated values of  $n_c$  at different temperatures are listed in Table 1. We notice that  $n_c$  is independent of temperature with an average value of  $1.93 \times 10^{21} \text{ cm}^{-3}$ . The temperature independence of  $n_c$  suggests that the mobility of  $\text{Li}^+$  ions is the factor that controls the conduction process in LBLT garnets in the investigated temperature range. It is interesting to compare the value of  $n_c$  with that of the total density  $N$  of  $\text{Li}^+$  ions. The value of  $N$  is calculated using the relation;  $N = m/V$ , where  $m$  is the number of lithium ions per unit cell ( $m = 48$  in LBLT) and  $V$  is the volume of the unit cell. Using an average value of the lattice parameter of  $12.9807 \text{ \AA}$  [4, 13, 14] gives a value of  $N = 2.2 \times 10^{22} \text{ cm}^{-3}$ . The percentage of the concentration of mobile  $\text{Li}^+$  ions,  $n_c$ , out of the total  $\text{Li}^+$  density,  $N$ , in LBLT garnets is only 8.79 %.

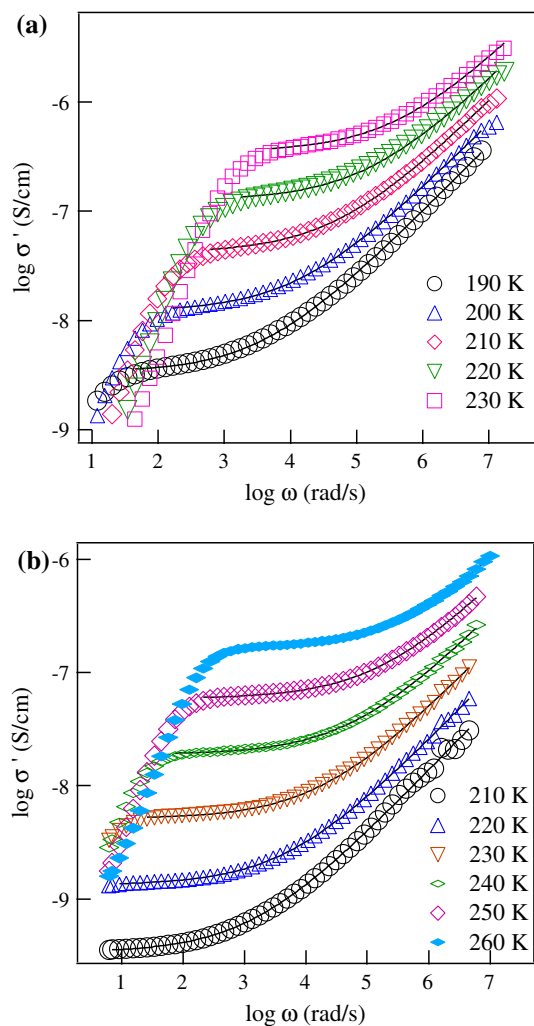


**Fig. 5** Conductivity spectra at selected temperatures for **a** LLBT-800 and **b** LLT-975 garnets. The *solid curves* between the *points* are the fits to Eq. (2)

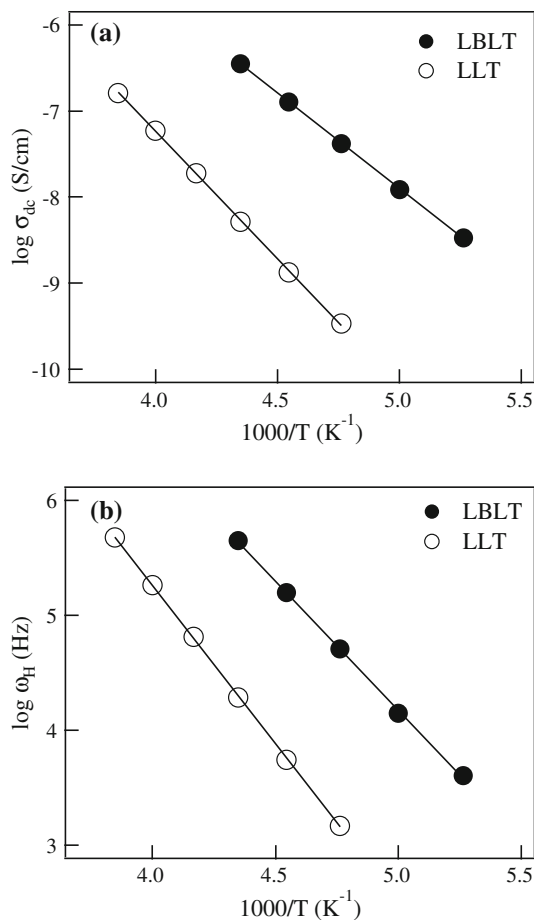


**Fig. 6** The temperature dependence of **a** the dc conductivity and **b** the hopping frequency determined from the fitting of the conductivity spectra for LBLT-800 and LLT-975 garnet materials

**Table 1** The dc conductivity  $\sigma_{dc}$ , the hopping frequency  $\omega_H$  and the power-law exponent  $n$  at different temperatures as determined from the fitting of the conductivity spectra

T (K)	$\sigma_{dc}$ (S/cm)	$\omega_H$ (Hz)	$n$	$n_c$ (cm <sup>-3</sup> )	$\mu$ (cm <sup>2</sup> /V s)	$D$ (cm <sup>2</sup> s <sup>-1</sup> )
<b>Li<sub>6</sub>BaLa<sub>2</sub>Ta<sub>2</sub>O<sub>12</sub></b>						
190	$3.36 \times 10^{-9}$	$4.02 \times 10^3$	0.61	$1.77 \times 10^{21}$	$1.18 \times 10^{-11}$	$1.93 \times 10^{-13}$
200	$1.22 \times 10^{-8}$	$1.40 \times 10^4$	0.60	$1.94 \times 10^{21}$	$3.91 \times 10^{-11}$	$6.74 \times 10^{-13}$
210	$4.19 \times 10^{-8}$	$5.09 \times 10^4$	0.60	$1.93 \times 10^{21}$	$1.36 \times 10^{-10}$	$2.45 \times 10^{-12}$
220	$1.27 \times 10^{-7}$	$1.58 \times 10^5$	0.60	$1.97 \times 10^{21}$	$4.00 \times 10^{-10}$	$7.59 \times 10^{-12}$
230	$3.53 \times 10^{-7}$	$4.47 \times 10^5$	0.60	$2.03 \times 10^{21}$	$1.09 \times 10^{-9}$	$2.15 \times 10^{-11}$
<b>Li<sub>5</sub>La<sub>3</sub>Ta<sub>2</sub>O<sub>12</sub></b>						
210	$3.38 \times 10^{-10}$	$1.47 \times 10^3$	0.57	$5.40 \times 10^{20}$	$3.91 \times 10^{-12}$	$7.07 \times 10^{-14}$
220	$1.33 \times 10^{-9}$	$5.48 \times 10^3$	0.56	$5.95 \times 10^{20}$	$1.40 \times 10^{-11}$	$2.65 \times 10^{-13}$
230	$5.14 \times 10^{-9}$	$1.93 \times 10^4$	0.55	$6.82 \times 10^{20}$	$4.70 \times 10^{-11}$	$9.32 \times 10^{-13}$
240	$1.92 \times 10^{-8}$	$6.83 \times 10^4$	0.56	$7.51 \times 10^{20}$	$1.59 \times 10^{-10}$	$3.29 \times 10^{-12}$
250	$6.10 \times 10^{-8}$	$2.16 \times 10^5$	0.58	$7.89 \times 10^{20}$	$4.83 \times 10^{-10}$	$1.04 \times 10^{-11}$

The mobility  $\mu$  and the diffusivity  $D$  are calculated from Eqs. (3) and (4), respectively



In order to understand the enhanced conductivity in LBLT compared to LLT, we have analyzed the conductivity spectra of LLT using Eq. (2) and the results are shown in Fig. 5b. The temperature dependence of  $\sigma_{dc}$  and  $\omega_c$  for LLT is also included in Fig. 6. The values of  $E_\sigma$  and  $E_H$  for LLT are 0.59 and 0.55 eV, respectively. The estimated values of  $n_c$  for LLT are listed in Table 1. Similar to LBLT, the values of  $n_c$  are found to be independent of temperature with an average value of  $6.71 \times 10^{20} \text{ cm}^{-3}$ . Using the value of the lattice parameter of 12.804 Å [5], then the total density  $N$  of  $\text{Li}^+$  ions is calculated to be  $1.91 \times 10^{22} \text{ cm}^{-3}$ . Therefore, the percentage of the mobile  $\text{Li}^+$  ions to the total density of  $\text{Li}^+$  ions in LLT is 3.52 %. The temperature dependence of the concentration,  $n_c$ , and mobility,  $\mu$ , of mobile  $\text{Li}^+$  ions in LBLT and LLT garnets is shown in Fig. 7.

The diffusivity of  $\text{Li}^+$  ions is related to the dc conductivity through the relation;

$$D = \frac{\sigma_{dc} kT}{n_c e^2} \tag{4}$$

The values of the mobility [calculated from Eq. (3)] and the diffusivity of  $\text{Li}^+$  ions are listed in Table 1 at different temperatures for LBLT and LLT samples. The values of  $D$  for both the LBLT and LLT could be compared to other Li superionic conductors. For example, the crystallized  $(\text{Li}_2\text{S})_7(\text{P}_2\text{S}_5)_3$  lithium ion conductor exhibits ionic conductivity value of  $3.86 \times 10^{-3} \text{ S/cm}$  and a diffusion coefficient of  $4.58 \times 10^{-8} \text{ cm}^2 \text{ s}^{-1}$  at 303 K [35]. The extrapolation of the diffusivity data of LBLT and LLT gives a value of  $D$  of  $4.79 \times 10^{-9}$  and  $9.71 \times 10^{-10} \text{ cm}^2 \text{ s}^{-1}$ , respectively, at 303 K. This value of  $D$  of LBLT is one order of magnitude smaller than that of the  $(\text{Li}_2\text{S})_7(\text{P}_2\text{S}_5)_3$  superionic conductor, whereas the value of  $D$  of LLT is even smaller. These differences in  $D$  are acceptable knowing that the ionic conductivity of LBLT and LLT are almost two and three orders of magnitude, respectively, smaller than that of  $(\text{Li}_2\text{S})_7(\text{P}_2\text{S}_5)_3$ .

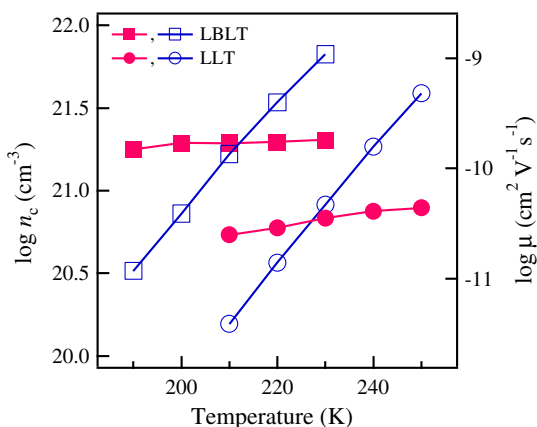


**Fig. 7** The temperature dependence of the concentration  $n_c$  (solid symbols) and the mobility  $\mu$  of mobile  $\text{Li}^+$  ions (open symbols) in LBLT-800 and LLT-975 garnets

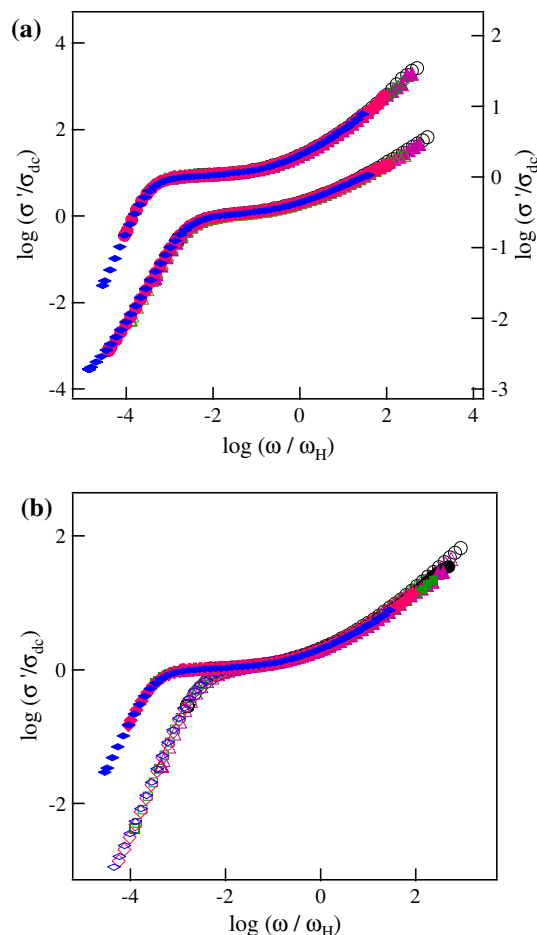


**Fig. 8** Scaling of the conductivity spectra for **a** the LLT-975 (upper curves) and LBLT-800 (lower curves) at different temperatures, and **b** for LLT-975 (solid symbols) and LBLT-800 (open symbols) garnets together at different temperatures

The above results confirm the following: (1) the total density of  $\text{Li}^+$  ions is already high in the range of  $1.91 \times 10^{22}$ – $2.2 \times 10^{22} \text{ cm}^{-3}$  in LLT and LBLT garnets, respectively; (2) not all  $\text{Li}^+$  ions contribute to the ionic conduction process in lithium garnet materials, but actually small fraction of  $\text{Li}^+$  ions are mobile; (3) the concentration of mobile  $\text{Li}^+$  ions is independent of temperature in LBLT and LLT and the conductivity behavior is controlled by the mobility of  $\text{Li}^+$  ions; (4) the ratio of  $n_c$  (LBLT)/ $n_c$  (LLT) is  $\sim 2.88$  at low temperatures, which cannot explain the 100-fold difference of the conductivity. Therefore the enhanced conductivity in LBLT is largely due to the increased mobility/diffusivity of  $\text{Li}^+$  ions as could be observed from Table 1 and Fig. 7; (5) the increased mobility of  $\text{Li}^+$  ions in LBLT garnets is due to the reduced occupancy of 24d tetrahedral sites, leading to accessible vacant sites for mobile  $\text{Li}^+$  ions and the formation of 3D pathways for  $\text{Li}^+$  ions diffusion. The recent study on  $\text{Li}_7\text{La}_3\text{Zr}_2\text{O}_{12}$   $\text{Li}^+$  conducting garnets supports the current results and conclusions [36].

Scaling of the conductivity spectra can represent a test of the universality of the dynamic response. We have scaled the conductivity spectra at different temperatures for LLT and LBLT in Fig. 8a, where  $\sigma_{dc}$  and  $\omega_H$  are used as the scaling parameters for the  $\sigma'$  and  $\omega$  axes, respectively. The conductivity spectra at different temperatures are found to superimpose properly into a single master curve, indicating that the relaxation dynamics of mobile  $\text{Li}^+$  ions are independent of temperature. The scaling results for LLT and LBLT garnets together are shown in Fig. 8b. It is observed that the conductivity spectra of both samples superimpose at the high frequency dispersion region indicating a common dynamics response. At the low frequency region, which represents electrode polarization effects, the conductivity spectra of LLT deviate from those of the LBLT garnet. These features may indicate that the electrode polarization depends on the density and mobility of mobile  $\text{Li}^+$  ions.

#### 4 Conclusions

$\text{Li}_6\text{BaLa}_2\text{Ta}_2\text{O}_{12}$  fine-grained ceramics have been obtained by low temperature sintering at 800 °C with a conductivity value of  $5.09 \times 10^{-5}$  S/cm at RT. With increasing sintering temperature to 900 °C coarse grained ceramics are obtained with slightly reduced conductivity. The enhanced conductivity of LBLT-800 than LBLT-900 is due to the enhanced mobility of  $\text{Li}^+$  ions in the fine-grained ceramics. The conductivity and the hopping frequency of  $\text{Li}^+$  ions in the studied garnet materials are thermally activated with the same activation energy, indicating that the concentration of mobile  $\text{Li}^+$  ions is independent of temperature with an average value of  $1.93 \times 10^{21}$  and  $6.71 \times 10^{20}$   $\text{cm}^{-3}$  for LBLT and LLT, respectively. With increasing the  $\text{Li}^+$  content per unit formula from 5 for LLT to 6 for LBLT the mobility as well as the concentration of mobile  $\text{Li}^+$  ions increase. However we have found that only a small fraction of  $\text{Li}^+$  ions of 3.52 and 8.79 % out of the total  $\text{Li}^+$  ions density for LLT and LBLT, respectively, are involved in the conduction process in the temperature range studied.

**Acknowledgments** The authors acknowledge the financial support from King Abdulaziz City for Science and Technology (KACST) under Grant No. ARP-30-109.

#### References

1. M. Armand, J.-M. Tarascon, *Nature* **451**, 652 (2008)
2. J. Hasoun, S. Panero, P. Reale, B. Scrosati, *Adv. Mater.* **21**, 1 (2009)
3. C.H. Chen, S. Xie, E. Sperling, A.S. Yang, G. Henriksen, K. Amine, *Solid State Ion.* **167**, 263 (2004)
4. V. Thangadurai, W. Weppner, *Adv. Funct. Mater.* **15**, 107 (2005)
5. V. Thangadurai, H. Kaack, W. Weppner, *J. Am. Ceram. Soc.* **86**, 437 (2003)
6. V. Thangadurai, W. Weppner, *J. Am. Ceram. Soc.* **88**, 411 (2005)
7. V. Thangadurai, W. Weppner, *J. Power Sources* **142**, 339 (2005)
8. R. Murugan, W. Weppner, P. Schmid-Beurmann, V. Thangadurai, *Mater. Sci. Eng., B* **143**, 14 (2007)
9. R. Murugan, V. Thangadurai, W. Weppner, *Angew. Chem. Int. Ed.* **46**, 7778 (2007)
10. E. Rangasamy, J. Wolfenstine, J. Sakamoto, *Solid State Ion.* **206**, 28 (2012)
11. S. Narayanan, V. Thangadurai, *J. Power Sources* **196**, 8085 (2011)
12. A.K. Baral, S. Narayanan, F. Ramezanipour, V. Thangadurai, *Phys. Chem. Chem. Phys.* **16**, 11356 (2014)
13. J. Awaka, N. Kijima, Y. Takahashi, H. Hayakawa, J. Akimoto, *Solid State Ion.* **180**, 602 (2009)
14. I. Kokal, K.V. Ramanujachary, P.H.L. Notten, H.T. Hintzen, *Mater. Res. Bull.* **47**, 1932 (2012)
15. Y. Li, J.T. Han, C.A. Wang, H. Xie, J.B. Goodenough, *J. Mater. Chem.* **22**, 15357 (2012)
16. S. Ohta, T. Kobayashi, T. Asaoka, *J. Power Sources* **196**, 3342 (2011)
17. Y. Li, C.A. Wang, H. Xie, J. Cheng, J.B. Goodenough, *Electrochem. Commun.* **13**, 1289 (2011)
18. S. Narayanan, V. Epp, M. Wilkening, V. Thangadurai, *RCS Adv.* **2**, 2553 (2012)
19. D. Pinzaru, V. Thangadurai, *J. Electrochem. Soc.* **161**, A2060 (2014)
20. S. Ramakumar, N. Janani, R. Murugan, *Dalton Trans.* **44**, 539 (2015)
21. M.G. Bellino, D.G. Lamas, N.E. Walsoe de Rica, *Adv. Mater.* **18**, 3005 (2006)
22. P. Heitjans, M. Masoud, A. Feldhoff, M. Wilkening, *Faraday Discuss.* **134**, 67 (2007)
23. E.J. Cussen, *Chem. Commun.* **4**, 412 (2006)
24. M.P. O'Challaghan, A.S. Powell, J.J. Titman, G.Z. Chen, E.J. Cussen, *Chem. Mater.* **20**, 2360 (2008)
25. L. Wullen, T. Echelmeyer, H.W. Meyer, D. Wilmer, *Phys. Chem. Chem. Phys.* **9**, 3298 (2007)
26. J. Han, J. Zhu, Y. Li, X. Yu, S. Wang, G. Wu, H. Xie, S.C. Vogel, F. Izumi, K. Momma, Y. Kawamura, Y. Huang, J.B. Goodenough, Y. Zhao, *Chem. Commun.* **48**, 9840 (2012)
27. R. Jalem, Y. Yamamoto, H. Shiiba, M. Nakayama, H. Munakata, T. Kasuga, K. Kanamura, *Chem. Mater.* **25**, 425 (2013)
28. M. Xu, M.S. Park, J.M. Lee, T.Y. Kim, Y.S. Park, E. Ma, *Phys. Rev. B* **85**, 052301 (2012)
29. M.P. O'Challaghan, E.J. Cussen, *Chem. Commun.* **20**, 2048 (2007)
30. M.M. Ahmad, K. Yamada, *J. Chem. Phys.* **127**, 124507 (2007)
31. E.F. Hairetdinov, N.F. Uvarov, H.K. Patel, S.W. Martin, *Phys. Rev. B* **50**, 13259 (1994)
32. A. Ghosh, A. Pan, *Phys. Rev. Lett.* **84**, 2188 (2000)
33. D.P. Almond, G.K. Ducan, A.R. West, *Solid State Ion.* **8**, 159 (1983)
34. S. Adams, R.P. Rao, *J. Mater. Chem.* **22**, 1426 (2012)
35. K. Hayamizu, Y. Aihara, *Solid State Ion.* **238**, 7 (2013)
36. M.M. Ahmad, *RSC Adv.* **5**, 25824 (2015)